HHS Public Access

Author manuscript

J Thorac Cardiovasc Surg. Author manuscript; available in PMC 2021 March 01.

Published in final edited form as:

J Thorac Cardiovasc Surg. 2020 March ; 159(3): 829–838.e3. doi:10.1016/j.jtcvs.2019.04.091.

MODELING RISK OF CORONARY OBSTRUCTION DURING TRANSCATHETER AORTIC VALVE REPLACEMENT

Megan Heitkemper[1], **Hoda Hatoum**[1], **Amirsepeher Azimian**[1], **Breandan Yeats**[1], **Jennifer Dollery**[3], **Bryan Whitson**[3], **Greg Rushing**[3], **Juan Crestanello**[1,3], **Scott M Lilly**[2], **Lakshmi Prasad Dasi**[1,3]

[1]Department of Biomedical Engineering, The Ohio State University, Columbus, OH USA

[2]Division of Cardiology, The Ohio State University, Columbus, OH USA

[3]Department of Surgery, The Ohio State University, Columbus, OH USA

Abstract

Objective: In this study we aim to evaluate risk of coronary obstruction during transcatheter aortic valve replacement (TAVR) and develop improved criteria based on computational modeling.

Methods: Patient specific 3D models were constructed and validated for 28 patients out of 600 that were flagged as high risk for coronary obstruction (defined as meeting coronary ostium height (*h)* < 14 mm and/or Sinus of Valsalva (*SOVd)* < 30 mm). The models consisted finite element analysis to predict the post-TAVR native cusp apposition relative to the coronary ostium and validated in-vitro. The distance from cusp to coronary ostium (*DLC*) was derived from the 3D models and indexed with the coronary artery diameter, *d* to yield a fractional obstruction measure (*DLC/d*)

Results: 22 out of 28 high risk patients successfully underwent TAVR without coronary obstruction and 6 did not. *DLC/d* between the two groups was significantly different ($p < 0.00078$) while neither *h* nor *SOVd* were significantly different ($p > 0.32$). A cut off of *DLC/d* < 0.7 was predictive with 100% sensitivity and 95.7% specificity. The optimal sensitivity and specificity of *h* and *SOVd* in this high risk group was only 60% and 40% respectively for a cut off *h* = 10 mm and *SOVd* of 30.5 mm.

Conclusions: 3D modeling has the potential to enable more patients be safely treated with TAVR who have low lying coronary ostium or small *SOVd*. *DLC/d* is more predictive of obstruction than *h* and *SOVd*.

Graphical Abstract

Address for correspondence and reprints: Lakshmi Prasad Dasi, PhD, Associate Professor, Department of Biomedical Engineering, Department of Surgery, The Ohio State University, Room 405A DHLRI, 473 W 12th Ave., Columbus, OH 43210, TEL: (614) 247-8313, FAX: (614) 292-9530, lakshmi.dasi@osumc.edu.

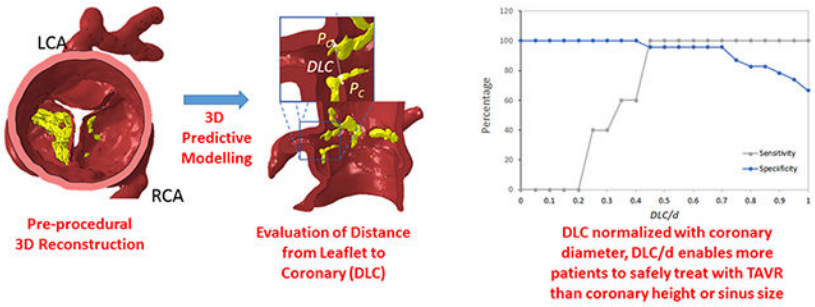

3D model-generated prediction of coronary obstruc-tion using the new DLC parameter.

Keywords

TAVR; Coronary Obstruction; Calcification; FEA; CFD; Patient-specific; [23] Catheter-based coronary and valvular interventions: other

1. Introduction:

Transcatheter aortic valve replacement (TAVR) represents a major advance in the field of cardiac surgery and interventional cardiology for the treatment of patients with severe aortic stenosis, whom conventional open-heart surgery has been deemed high risk (1–4). Despite the overall effectiveness of TAVR, complications can limit the realization of mortality and quality of life benefits (4–7). Among these is coronary obstruction, which can occur upon transcatheter valve deployment, and most often affects the left coronary artery (LCA) (8–15). Coronary obstruction, as defined by the 2011 ACCF/AHA/SCAI guidelines for percutaneous coronary intervention, is considered as a > 50% obstruction of the left main coronary artery, >70% in any other coronary artery, or both (16,17). While this complication is rare (reported in up to 1% of all TAVR procedures) the outcomes can often be catastrophic.

Although a serious and potentially preventable complication, there is no consensus to which features reliably predispose risk of coronary obstruction during TAVR. Most of the guidelines developed so far have originated from clinical trials designed to exclude as many adverse outcomes as possible and were not based on simulations or mechanistic insights into the precise mechanics of coronary obstruction. In doing so, these guidelines have potential to exclude a large number of potential TAVR patients, often those who have no other treatment options available.

Despite the existing predictive models, 1-3% of TAVR patients still suffer from coronary obstruction. However, it has been shown that restrictively applying the current guidelines could have excluded 26 - 33% of patients who successfully received TAV with no reported instance of coronary obstruction (29). This clearly demonstrates the importance of patient specific modeling and the critical need for individualization of valve replacement therapy.

The objective of this study is to better understand the physical mechanism of coronary obstruction beyond the conventional parameters of h and $SOVd$ alone and introduce a new

more accurate mechanistic index that can predict which high risk patients (i.e. patients with $h < 14$ mm and/or $SOVd < 30$mm) are not actually at risk and are indeed candidates for TAVR pre-operatively, allowing for the most patients possible to safely undergo TAVR without coronary obstruction.

2. Methods:

In order to better understand the mechanism of coronary obstruction and develop a mechanistic index that can predict which high risk patients (i.e. patients with $h < 14$ mm and/or $SOVd < 30$mm) are not actually at risk and are indeed candidates for TAVR pre-operatively, a three-dimensional computational model that utilize pre-TAVR CT angiogram imaging is presented and compared against the conventional guidelines. The three-dimensional model employs computer-aided methodologies that predict the closest distance between native aortic valve cusp and the corresponding coronary artery ostium following TAV deployment. In vitro validation of this novel computational model was performed using 3D printed flexible patient specific aortic root geometries. Informed consent was obtained from all patients and the study complied with the Institutional Review Board of The Ohio State University.

2.1 Study Population:

The study population included all “moderate to high-risk” patients, defined by left coronary artery height ($LCAh$) < 14 mm and/or $SOVd < 30$ mm, flagged from 600 aortic stenosis patients considered for TAVR at The Ohio State University Wexner Medical Center between January 2014 and September 2018. This filtering resulted in 28 patients (labeled A-AB; see Table 1) being flagged as moderate to high risk for left coronary artery obstruction during TAVR and included 78.5% women; mean [± SD] age, 80 ± 9 years with symptomatic severe aortic stenosis. The individual $LCAh$ and $SOVd$ are shown in Figure 1 for the study population with quadrants representing $LCAh < 12$ mm and $SOVd < 30$ mm based on Ribeiro et. al’s analysis as current guidelines (the figure is discussed later).

With respect to the outcomes for these 28 patients, 23 received TAVR successfully while 5 patients did not receive a successful TAVR. These five include 1 male who suffered coronary obstruction (presented in supplementary material Video S1), 2 females who underwent surgical aortic valve replacement with visual confirmation of coronary obstruction by the operating surgeon, and 1 male and 1 female (patients H and V) who each had extremely low lying coronary ostium (9mm and 7.6mm respectively) and were deemed surgically inoperable due to age and received medical management.

2.2 Three-dimensional (3D) Computational Model:

A 3D computational model was developed to assess risk of coronary obstruction during TAVR. Note that this model is only for patients who already satisfy a conservative risk stratification given by $h < 14$ mm and/or $SOVd < 30$ mm and as is shown later that there would not be any benefit to perform 3D computational modeling for lower risk patients. The model works by simulating the implantation of an idealized and cylindrical TAV prosthesis into a patient’s pre-procedural aortic root anatomy (including the calcified native cusps). The

risk for coronary obstruction is then assessed through quantifying the closest distance of the cusp and the corresponding coronary ostium. This distance is indexed to the coronary artery diameter to obtain a representative measure of the fractional obstruction of the native cusp "eclipsing" the ostium.

The pre-procedural patient specific aortic root, calcium nodules and cusps were segmented for each of the 28 patients from pre-TAVR CT images using Mimics Research 18.0 (Materialise, Belgium). The segmented aortic wall, cusps and calcium nodules were then discretized in 3-Matic Research 13.0 (Materialise, Belgium) using explicit 4-node linear tetrahedron elements (Supplementary Figure S1). An idealized TAV stent (represented as an expandable cylinder) was discretized using hexahedral elements.

An example of the segmented aortic root (red) and cusp with calcification (yellow) anatomy previous to TAV implantation is depicted in Figure 2A,B,C. Finite element analysis (FEA) was performed on each patient-specific 3D anatomical model using Abaqus/Explicit 6.9 software (Simulia, Providence, RI, USA) to simulate the opening of a TAV device stent that pushes the native cusps open towards the coronary ostium. For each patient anatomy, the simulation expanded the TAV device stent to the diameter of the valve size that would be appropriate for that patient's anatomy, as determined by the structural heart team at Ohio State University Wexner Medical Center. The simulated TAV expanded diameters and the valve sizes received are given in Table 1. Material properties of the pressurized aortic root were assigned using an isotropic neo-Hookean hyper-elastic model based on the studies by Bosmons et al. (2016), Auricchio et al. (2014), and Martin et al. (2012). The strain energy function is described below.

$$W = \frac{\mu}{2}(I_1 - 3 - 0.5\ Ln\ J) + \frac{\lambda}{2}(Ln\ J)^2$$

Which μ and λ are shear and bulk modulus respectively and are shown in Supplementary Table T1 for each part. Calcium nodules were approximated to be linear elastic. The Young's modulus was based on the nonlinear elastic material properties introduced by Billiar and Sacks (30).

Figure 2D shows a schematic of the post simulation anatomy highlighting the closest distance between the left cusp (point P_C in the figure) and corresponding coronary ostium (point P_O) denoted as *DLC*. *DLC* represents the predicted gap in mm as would be seen in a long axis plane showing both the coronary ostium and the native cusp. Figure 2E and 2F show different three dimensional perspectives of the post simulation anatomy for the same distance (*DLC*) from a cross sectional and top view for the same patient. *DLC* was then normalized with respect to the corresponding coronary artery diameter (*d*), to obtain *DLC/d,* which represents the fraction of distance between the aortic cusp and coronary ostium post TAV deployment available for blood flow towards the coronary ostium. A fractional value greater than unity indicates that the gap available for blood flow is greater than the coronary artery diameter. A fractional value approaching zero indicates total occlusion. Supplementary Figure S2 visualizes the same for four patients.

2.3 In Vitro Validation:

The computational model was validated in-vitro as well as in-vivo. Two flexible patient-specific 3D printed models of aortic root geometries, the first with 3D printed patient calcium nodules, and the second without calcium nodules, were used to evaluate the potential effects of rigid calcium nodules on cusps' deformation during TAVR. The 3D printed aortic root model was manufactured using Connex 350 3D printer (Stratasys, Eden Prairie, MN) from TangoPlus material for the aorta and cusps with VeroWhite material used for the calcium nodules (Figure 3). The flexible 3D printed model with the calcification nodules itself was also validated, through comparison of patient hemodynamics (peak gradients and velocities) with experimental values obtained from left heart flow simulator studies (31,32). An idealized tool (Figure 3F) was used to open the cusps to the appropriate stent size for the 3D printed models and was compared against the results of the FEA simulation of the same patient with and without inclusion of calcium nodules. As shown in Supplementary Figure S3 there was excellent agreement between the computational prediction and experimental measurements of *DLC*.

Further validation of the 3D computational approach was achieved with the observation of coronary occlusion to occur in two patients (J and T in Table 1) as predicted by the model and confirmed by the operating surgeon during surgical AVR.

2.4 Statistical Analysis:

A Mann-Whitney non parametric comparison of means was performed for each of the three parameters (*DLC/d*, *h*, and *SOVd*) to compare the mean parameter value between the two groups; the 23 that received TAVR successfully and the 5 patients that did not receive a successful TAVR. A sensitivity and specificity analysis was performed for each test (*DLC/d*, *h*, and *SOVd*) by identifying how many patients would identify as true positive, false positive, true negative or false negative for coronary obstruction under a range of cutoff values. Sensitivity is then calculated as:

$$Sensitivity = \frac{True\ positives}{True\ positives + False\ negatives},$$

While specificity is calculated as:

$$Specificity = \frac{True\ negatives}{True\ negatives + False\ positives},$$

as described in Lalkhen and McCluckey (2008) (33).

3. Results:

Here we present results that compare the ability of solely conventional parameters such as *h* and *SOVd* and the new parameter *DLC/d* to differentiate which high risk patients are not actually at risk and are indeed candidates for TAVR. Routine anatomical measurements of *h* and *SOVd* along with measured values from the 3D computational model, *DLC* and *DLC/d*, for the high risk study population (28 patients) are presented in Table 1.

3.1 Current guidelines (*h,SOVd*):

Figure 1 shows the risk assessment for left coronary obstruction occurrence under the existing guidelines (i.e. $h < 12$ and $SOVd < 30mm$) based on Ribeiro *et. al* (18). Obstruction of the right coronary artery was not evaluated due to lack of right coronary obstruction in our patient population. Accordingly left coronary obstruction was expected to occur for 22 of the 28 patients, with left *SOVd* in the range 26.0-36.2 (mm) and left coronary artery height (*LCAh*) in the range of 7.09-19.0 (mm).

3.2 3D predictive model (*DLC/d*):

The distribution of *DLC/d* among the patient population is shown in Figure 4. The range of values for *DLC/d* for the patients is between 0.0203 and 3.89. The horizontal line between 0.5 and 0.7 approximately separates patients who successfully received TAVR (above the line) from those who did not. The one blue data point that lies just below the horizontal line successfully received TAVR but only with coronary protection using a stent.

3.3 Comparison to current guidelines:

The mean and standard deviations of the parameter values for those high risk patients who successfully received TAVR without coronary obstruction are compared to those who did not receive TAVR successfully in Figure 5. The means for these two groups were compared using a Mann-Whitney non parametric test, and the only significant difference between the two groups was found for the *DLC/d* parameter, with $p < 0.00078$. Neither *LCAh* nor *SOVd* was significantly different between the two groups with $p = 0.35238$ and $p = 0.32218$ respectively.

Figure 6 shows sensitivity and specificity curves generated for each of the three parameters to accurately predict whether TAVR within this high risk patient population would not be successful. Figure 6A shows that the sensitivity of *LCAh* increases steadily from 0% at an *LCAh* cutoff of 7 mm to a 100% sensitivity at *LCAh* cutoff at 12 mm. Specificity of *LCAh* on the other hand drops steadily from 100% at 7mm to 0% at a cutoff of 19 mm. The crossover point for sensitivity and specificity for *LCAh* as an optimal predictor of coronary obstruction was at $LCAh = 10mm$ with approximately 60% sensitivity and specificity. The sensitivity and specificity of *SOVd* as an independent predictor of unsuccessful TAVR is shown in Figure 6B. The sensitivity increases from 0% at *SOVd* of 28mm to 100% at 38mm. Specificity drops from 100% at 26mm to 0% at 38mm. The optimal crossover point occurs approximately at 30.5mm with a sensitivity and specificity of 40%. With respect to sensitivity and specificity of the 3D computational parameter *DLC/d* (Figure 6C), the sensitivity is 0% at a value of 0.2 and increases to 100% at a value of 0.45. The specificity drops from 100% at a value of 0.4 to 66% at a value of 1.0. The optimal crossover point is slightly below 0.45 with a sensitivity and specificity of 96%. There is a range of *DLC/d* from 0.45 to 0.70 for which the sensitivity and specificity exceed 95%.

4. Discussion:

Although the prevalence of coronary obstruction during TAVR procedure is rather low (< 1%), it is a time-sensitive and life-threatening complication. In order to minimize cases of

coronary obstruction after TAV deployment, studies have introduced safety guidelines that attempt to use geometrical factors of patient aortic root geometry prior to implantation to assess patient risk (19–22,29,34). In one such study, Ribeiro *et. al.* reported that the average coronary artery height (*h*) and mean sinus of Valsalva diameter (*SOVd*) were smaller for patients that suffered coronary obstruction during TAVR(18). These concepts were applied to a large population of patients that underwent TAVR (n = 6688, 44 with coronary obstruction) and standard parameters indicating the potential for coronary obstruction were suggested as follows: 1) $h < 12$ mm, 2) $SOVd < 30$ mm (18). In a smaller observational study Yamamoto *et al.* (19) examined 666 cases of TAVR (10 with coronary obstruction), and created their own criteria for potential risk: 1) $h < 10$ mm, 2) valve cusp length greater than *h*, and 3) shallow *SOV* (*SOVd* = 28.5 mm) with massive calcification. Although both of these reports suggest *h* and *SOVd* are important, other features are likely overlooked. The effect of the calcific nodules, for example, was not considered as a main anatomic predictor of coronary obstruction (18). Tops et al. (2008), Apfaltrer *et al.* (2011), and Binder et al. (2013) suggested noninvasive evaluation of aortic root using multi-slice CT (MSCT), aortoiliac CT, multidetector CT (MDCT), and three-dimensional modeling to provide more precise information on how aortic root geometry could play a role in complications such as coronary obstruction and paravalvar leakage.(20–22) Additional studies have focused on computational modeling using finite element analysis (FEA) as a powerful tool to optimize pre-operative planning of TAVR and evaluate its adverse outcomes in patient-specific geometries (23–28).

Not only have we shown that these safety guidelines that attempt to use geometrical features of patient's aortic roots prior to implantation are not always accurate in flagging patients with risk of coronary obstruction, but also that they significantly reduce the number of patients who could have safely undergone TAVR without coronary obstruction.

In this study, we evaluate the predictive capacity of existing methods and propose a novel method for the investigation of coronary obstruction risk in patients with severe aortic stenosis prior to TAVR who were flagged as at risk based on conventional predictive guidelines. The novel method utilizes 3D reconstructed patient geometry for simulation of TAV deployment using FEA. The current guidelines for high risk of coronary obstruction include *SOVd* less than 30 mm (18) and coronary ostium height (*h*) greater than 12 (mm) (35,36), although these guidelines are not consistently recognized throughout US hospitals. Individual transcatheter valve manufacturers impose their own guidelines, for example, CoreValve Evolut R & PRO manufacturers suggest that *SOVd* of ≥ 27 mm and ≥ 29 mm should be included (for the 26-mm and 29-mm Evolut R & PRO respectively). Similar to the *SOVd* guideline, coronary height $h \geq 14$ is recommended by the CoreValve Evolut R & PRO manufacturers. The latter guideline would exclude all but two of the patients in this study population, many of whom who safely underwent TAVR without coronary obstruction. On the other hand, the patient specific 3D predictive model captures a much more accurate representation of the TAVR procedure and would capture the final configuration of TAV stent along with native cusp and aortic wall precisely. Based on our findings, the parameter $DLC/d > 0.7$ when $h < 14$ mm and/or $SOVd < 30$ mm should be considered as patients who are not actually high risk for left coronary obstruction and patients who have $DLC/d < 0.5$ are at severe risk of coronary obstruction and TAVR should not be attempted in these

patients. Further studies are needed to resolve the patients where *DLC/d* lies between 0.5 and 0.7. Until then, these patients should be approached with caution with potential coronary protection strategies. Further, for patients with $h > 14$ mm and $SOVd > 30$ mm, there does not seem to be any benefit to perform simulations to evaluate *DLC/d* because there is no known case of coronary obstruction in this group and furthermore the objective of the new computational model is not to replace the current guidelines but to only augment the predictive power.

5. Limitation:

In this study we are not looking at coronary obstruction from conduit of TAV, which can occur due to mal-positioning (supra-annular) of TAV. Additionally, right coronary obstruction is not evaluated, since obstruction of right coronary is much less prevalent compared to left coronary (8–10). However, the 3D model is likely applicable to right coronary artery for pre-operative risk assessment of coronary obstruction. Another limitation of the study is the small number of cases evaluated for coronary obstruction, which is due to its relatively rare occurrence.

6. Conclusion:

We have successfully developed a highly accurate model to screen patients for possible coronary obstruction during TAVR based on criteria that can be readily calculated from current pre-TAVR CT angiographic imaging utilizing 3D FEA analysis. Neither h nor $SOVd$ is predictive of coronary obstruction when considering high risk patients with $h < 14$ mm and/or $SOVd < 30$mm. However, the new parameter *DLC/d* is predictive of coronary obstruction for the same high risk group. The performance of *DLC/d* was validated in-vitro and clinically. Results indicate that a significantly high fraction of patients who have $h < 14$ mm and/or $SOVd < 30$mm can be safely treated with TAVR if assessed with *DLC/d* as compared to the current guidelines using $SOVd$ and h alone. These findings shed light on a rare but significant potential complication during TAVR, and can assist heart teams in the decision-making process prior to the TAVR procedure.

Supplementary Material

Refer to Web version on PubMed Central for supplementary material.

Acknowledgments

Disclosures:

Dr. Juan Crestanello reports having grants from Medtronic, Boston Scientific and Abbot in addition to being part of the advisory board of Medtronic. Dr. Dasi and Megan Heitkemper report having two patents filed on novel polymeric heart valves. Dasi and Azimian also have a patent filed on 3D computational modeling for TAVR. No other conflicts were reported.

References:

1. Leon MB, Smith CR, Mack MJ et al. Transcatheter or surgical aortic-valve replacement in intermediate-risk patients. New England Journal of Medicine 2016;374:1609–1620. [PubMed: 27040324]
2. Masson J-B, Kovac J, Schuler G et al. Transcatheter aortic valve implantation: review of the nature, management, and avoidance of procedural complications. JACC: Cardiovascular Interventions 2009;2:811–820. [PubMed: 19778768]
3. Smith CR, Leon MB, Mack MJ et al. Transcatheter versus surgical aortic-valve replacement in high-risk patients. New England Journal of Medicine 2011;364:2187–2198. [PubMed: 21639811]
4. Dasi LP, Hatoum H, Kheradvar A et al. On the Mechanics of Transcatheter Aortic Valve Replacement. Annals of Biomedical Engineering 2016:1–22. [PubMed: 26620776]
5. Rodés-Cabau J Transcatheter aortic valve implantation: current and future approaches. Nature Reviews Cardiology 2012;9:15.
6. Dvir D, Leipsic J, Blanke P et al. Coronary Obstruction in Transcatheter Aortic Valve-in-Valve Implantation. Preprocedural Evaluation, Device Selection, Protection, and Treatment 2015;8.
7. Gurvitch R, Tay EL, Wijesinghe N et al. Transcatheter aortic valve implantation: lessons from the learning curve of the first 270 high-risk patients. Catheterization and cardiovascular interventions: official journal of the Society for Cardiac Angiography & Interventions 2011;78:977–984. [PubMed: 21656647]
8. Mizote I, Conradi L, Schäfer U. A case of anomalous left coronary artery obstruction caused by lotus valve implantation. Catheterization and Cardiovascular Interventions 2016.
9. Gökdeniz T, Aykan AÇ, Ağaç MT, Dağdelen S, Çelik Ş. Concomitant complete atrioventricular block and left main coronary artery occlusion during transcatheter aortic valve implantation. Heart, Lung and Circulation 2013;22:1048–1050.
10. Dağdelen S, Karabulut H, Alhan C. Acute left main coronary artery occlusion following TAVI and emergency solution. Anadolu kardiyoloji dergisi: AKD= the Anatolian journal of cardiology 2011;11:747. [PubMed: 22137950]
11. Zierer A, Wimmer-Greinecker G, Martens S, Moritz A, Doss M. The transapical approach for aortic valve implantation. The Journal of thoracic and cardiovascular surgery 2008;136:948–953. [PubMed: 18954635]
12. Flecher EM, Curry JW, Joudinaud TM, Kegel CL, Weber PA, Duran CM. Coronary flow obstruction in percutaneous aortic valve replacement. An in vitro study. European journal of cardio-thoracic surgery 2007;32:291–295. [PubMed: 17561412]
13. Gurvitch R, Cheung A, Bedogni F, Webb JG. Coronary obstruction following transcatheter aortic valve-in-valve implantation for failed surgical bioprostheses. Catheterization and Cardiovascular Interventions 2011;77:439–444. [PubMed: 21328685]
14. Bagur R, Dumont E, Doyle D et al. Coronary ostia stenosis after transcatheter aortic valve implantation. JACC: Cardiovascular Interventions 2010;3:253–255. [PubMed: 20170886]
15. Crimi G, Passerone G, Rubartelli P. Trans - apical aortic valve implantation complicated by left main occlusion. Catheterization and Cardiovascular Interventions 2011;78:656–659. [PubMed: 21656648]
16. Maddox TM, Stanislawski MA, Grunwald GK et al. Nonobstructive coronary artery disease and risk of myocardial infarction. JAMA 2014;312:1754–1763. [PubMed: 25369489]
17. Levine GN, Bates ER, Blankenship JC et al. 2011 ACCF/AHA/SCAI Guideline for Percutaneous Coronary Intervention: A Report of the American College of Cardiology Foundation/American Heart Association Task Force on Practice Guidelines and the Society for Cardiovascular Angiography and Interventions. Journal of the American College of Cardiology 2011;58:e44–e122. [PubMed: 22070834]
18. Ribeiro HB, Webb JG, Makkar RR et al. Predictive factors, management, and clinical outcomes of coronary obstruction following transcatheter aortic valve implantation: insights from a large multicenter registry. Journal of the American College of Cardiology 2013;62:1552–1562. [PubMed: 23954337]

19. Yamamoto M, Shimura T, Kano S et al. Impact of preparatory coronary protection in patients at high anatomical risk of acute coronary obstruction during transcatheter aortic valve implantation. International journal of cardiology 2016;217:58–63. [PubMed: 27179209]
20. Apfaltrer P, Schymik G, Reimer P et al. Aortoiliac CT angiography for planning transcutaneous aortic valve implantation: aortic root anatomy and frequency of clinically significant incidental findings. American Journal of Roentgenology 2012;198:939–945. [PubMed: 22451564]
21. Binder RK, Webb JG, Willson AB et al. The impact of integration of a multidetector computed tomography annulus area sizing algorithm on outcomes of transcatheter aortic valve replacement: a prospective, multicenter, controlled trial. Journal of the American College of Cardiology 2013;62:431–438. [PubMed: 23684679]
22. Tops LF, Wood DA, Delgado V et al. Noninvasive evaluation of the aortic root with multislice computed tomography: implications for transcatheter aortic valve replacement. JACC: Cardiovascular Imaging 2008;1:321–330. [PubMed: 19356444]
23. Auricchio F, Conti M, Morganti S, Reali A. Simulation of transcatheter aortic valve implantation: a patient-specific finite element approach. Computer methods in biomechanics and biomedical engineering 2014;17:1347–1357. [PubMed: 23402555]
24. Bosmans B, Famaey N, Verhoelst E, Bosmans J, Vander Sloten J. A validated methodology for patient specific computational modeling of self-expandable transcatheter aortic valve implantation. Journal of biomechanics 2016;49:2824–2830. [PubMed: 27395760]
25. Capelli C, Bosi G, Cerri E et al. Patient-specific simulations of transcatheter aortic valve stent implantation. Medical & biological engineering & computing 2012;50:183–192. [PubMed: 22286953]
26. Capelli C, Taylor AM, Migliavacca F, Bonhoeffer P, Schievano S. Patient-specific reconstructed anatomies and computer simulations are fundamental for selecting medical device treatment: application to a new percutaneous pulmonary valve. Philosophical Transactions of the Royal Society of London A: Mathematical, Physical and Engineering Sciences 2010;368:3027–3038.
27. Morganti S, Conti M, Aiello M et al. Simulation of transcatheter aortic valve implantation through patient-specific finite element analysis: two clinical cases. Journal of biomechanics 2014;47:2547–2555. [PubMed: 24998989]
28. Wang Q, Sirois E, Sun W. Patient-specific modeling of biomechanical interaction in transcatheter aortic valve deployment. Journal of biomechanics 2012;45:1965–1971. [PubMed: 22698832]
29. Ribeiro HB, Webb JG, Makkar RR et al. Predictive factors, management, and clinical outcomes of coronary obstruction following transcatheter aortic valve implantation: insights from a large multicenter registry. J Am Coll Cardiol 2013;62:1552–62. [PubMed: 23954337]
30. Billiar KL, Sacks MS. Biaxial mechanical properties of the natural and glutaraldehyde treated aortic valve cusp—part I: experimental results. Journal of biomechanical engineering 2000;122:23–30. [PubMed: 10790826]
31. Hatoum H, Dollery J, Lilly SM, Crestanello J, Dasi LP. Impact of patient-specific morphologies on sinus flow stasis in transcatheter aortic valve replacement: An in vitro study. The Journal of Thoracic and Cardiovascular Surgery.
32. Hatoum H, Yousefi A, Lilly S, Maureira P, Crestanello J, Dasi LP. An in vitro evaluation of turbulence after transcatheter aortic valve implantation. The Journal of Thoracic and Cardiovascular Surgery 2018;156:1837–1848. [PubMed: 29961588]
33. Lalkhen AG, McCluskey A. Clinical tests: sensitivity and specificity. Continuing Education in Anaesthesia Critical Care & Pain 2008;8:221–223.
34. Akhtar M, Tuzcu EM, Kapadia SR et al. Aortic root morphology in patients undergoing percutaneous aortic valve replacement: evidence of aortic root remodeling. The Journal of thoracic and cardiovascular surgery 2009;137:950–956. [PubMed: 19327523]
35. Achenbach S, Delgado V, Hausleiter J, Schoenhagen P, Min JK, Leipsic JA. SCCT expert consensus document on computed tomography imaging before transcatheter aortic valve implantation (TAVI)/transcatheter aortic valve replacement (TAVR). Journal of Cardiovascular Computed Tomography 2012;6:366–380. [PubMed: 23217460]

36. Holmes DR Jr, Mack MJ, Kaul S et al. 2012 ACCF/AATS/SCAI/STS Expert Consensus Document on Transcatheter Aortic Valve Replacement. Journal of the American College of Cardiology 2012;59:1200–1254. [PubMed: 22300974]

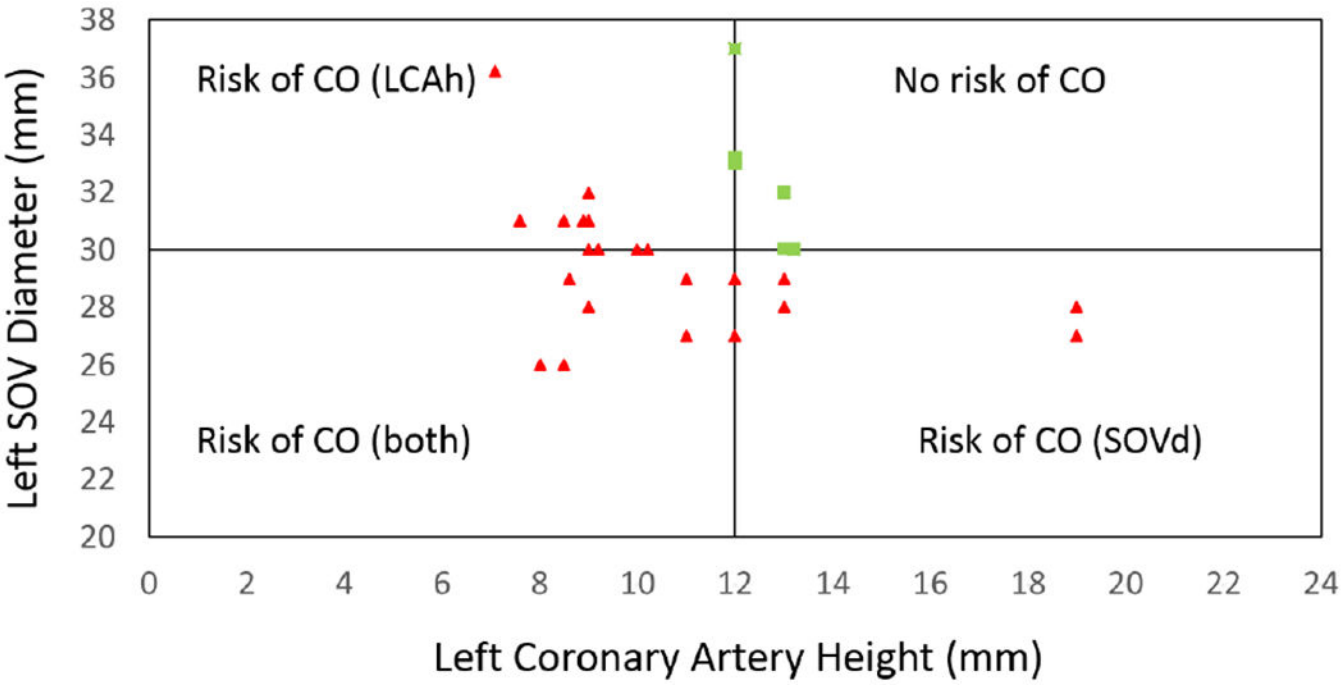

Figure 1.

Study population characterized by conventional parameters (coronary height (*h*) < 14 mm and Sinus of Valsalva diameter (*SOVd*) < 30 mm) used to predict left coronary artery obstruction prior to transcatheter aortic valve replacement (TAVR) with origin located at (12,30); Green squares represent the only patients who would have been approved for TAVR under these current guidelines.

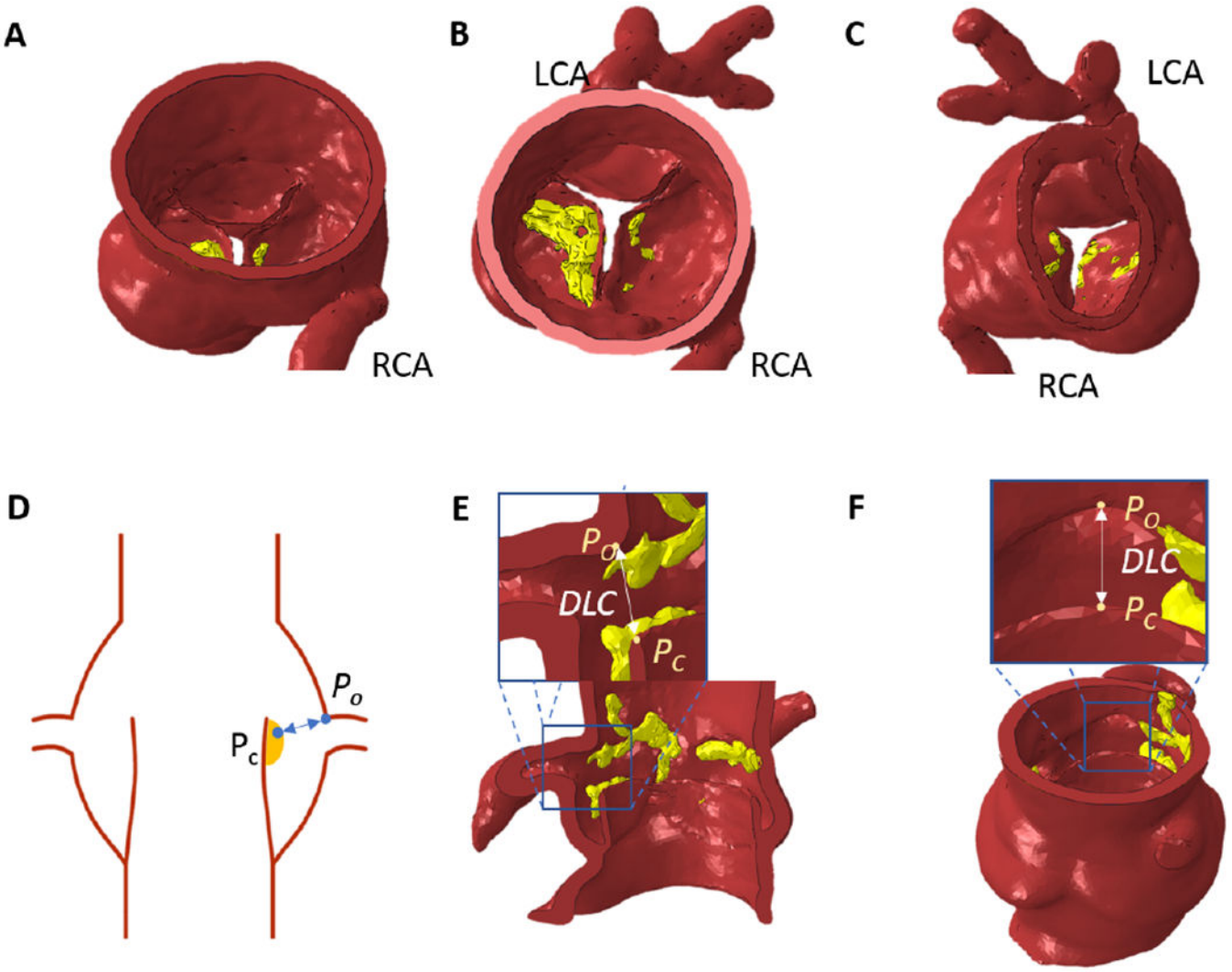

Figure 2.

Example of patient specific 3D modeled aortic root with left coronary artery (LCA), right coronary artery (RCA), and yellow calcific nodules; (A) side view (B) aortic view (C) ventricular view; The measured distance from a point on cusp/or cusp calcium (Pc) to a point on the upper ostium of the coronary artery (Po) following a transcatheter valve replacement (*DLC*) from (D) Idealized root schematic from the side view; example finite element simulated post-TAVR aortic root with *DLC* from a top view (E) and side view (F)

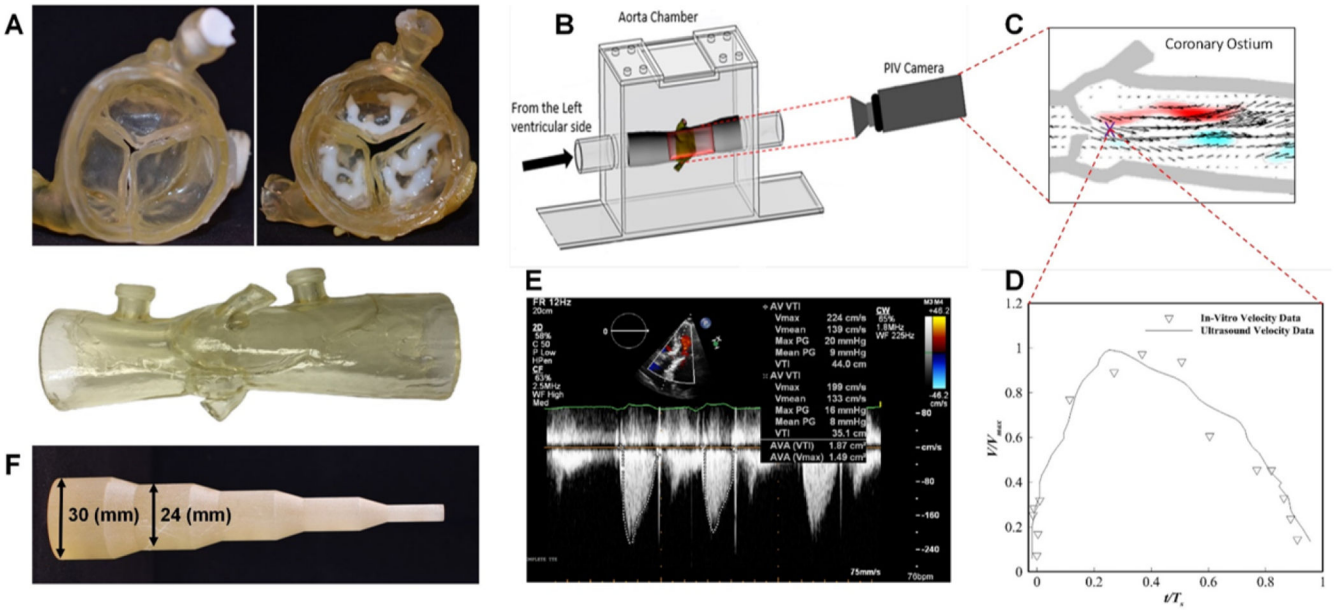

Figure 3.

The 3D printed aortic root model was manufactured from TangoPlus material, VeroWhite material was used for calcium nodule, both printed using Connex 350 3D printer (Stratasys, Eden Prairie, MN) (Figure 3, A). Particle image velocimetry (PIV) experiments (Figure 3, B) were performed to validate the 3D printed calcified aortic root model and compare with in-vivo ultrasound Doppler jet velocity for the patient. Detailed methodology of the PIV experiments may be found in literature 1. Comparison of the temporal velocity profile corresponding to a point located at the exit of the systolic jet of the valve (Figure 3, C) with Doppler data is shown in (Figure 3, D and E). As can be seen, the result shows good agreement between the in-vivo and in-vitro data. The maximum velocity in the PIV data was found to be 2.10 m/s which compares well with 2.24 m/s obtained from the ultrasound. Expansion tool with increasing diameter, which mimics balloon expansion (Figure 4, F).

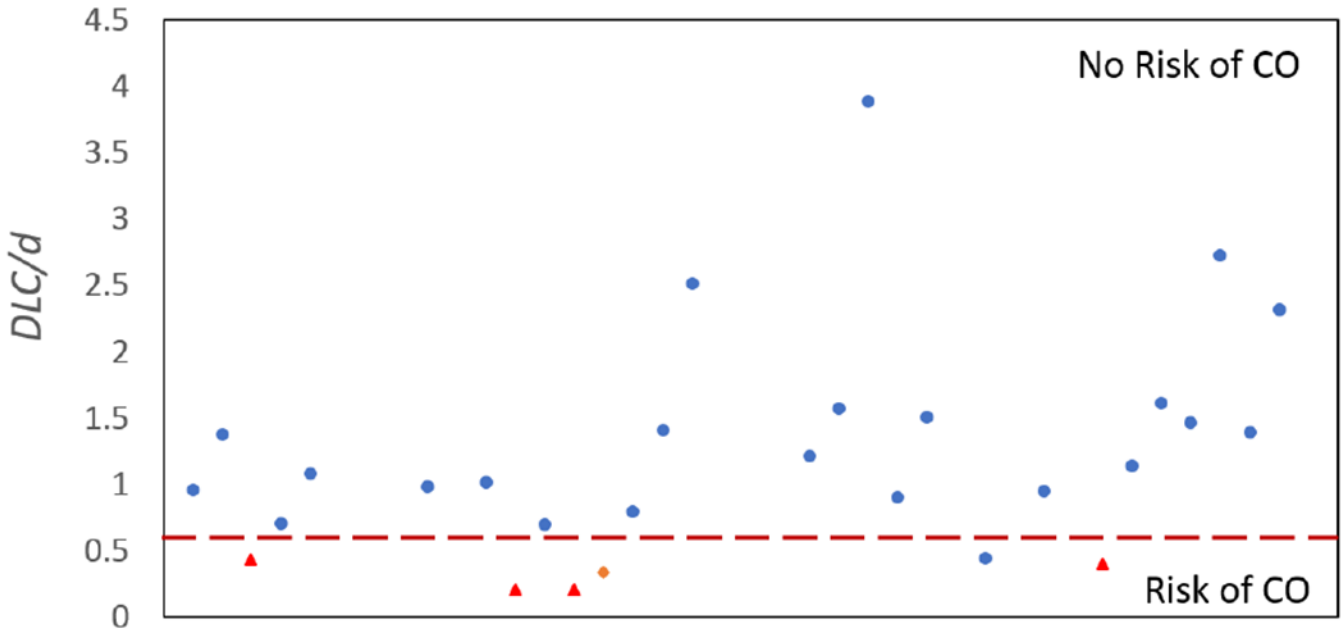

Figure 4.

Study population characterized by 3D predictive model (*DLC/d* < 0.7) used to predict left coronary artery obstruction prior to transcatheter aortic valve replacement; Blue dots represent the patients who were be approved for transcatheter aortic valve replacement under these suggested guidelines, red triangles represent those who were not approved and received other treatment, and the orange diamond represents the one patient where transcatheter aortic valve replacement resulted in coronary obstruction (the model was not computed prior).

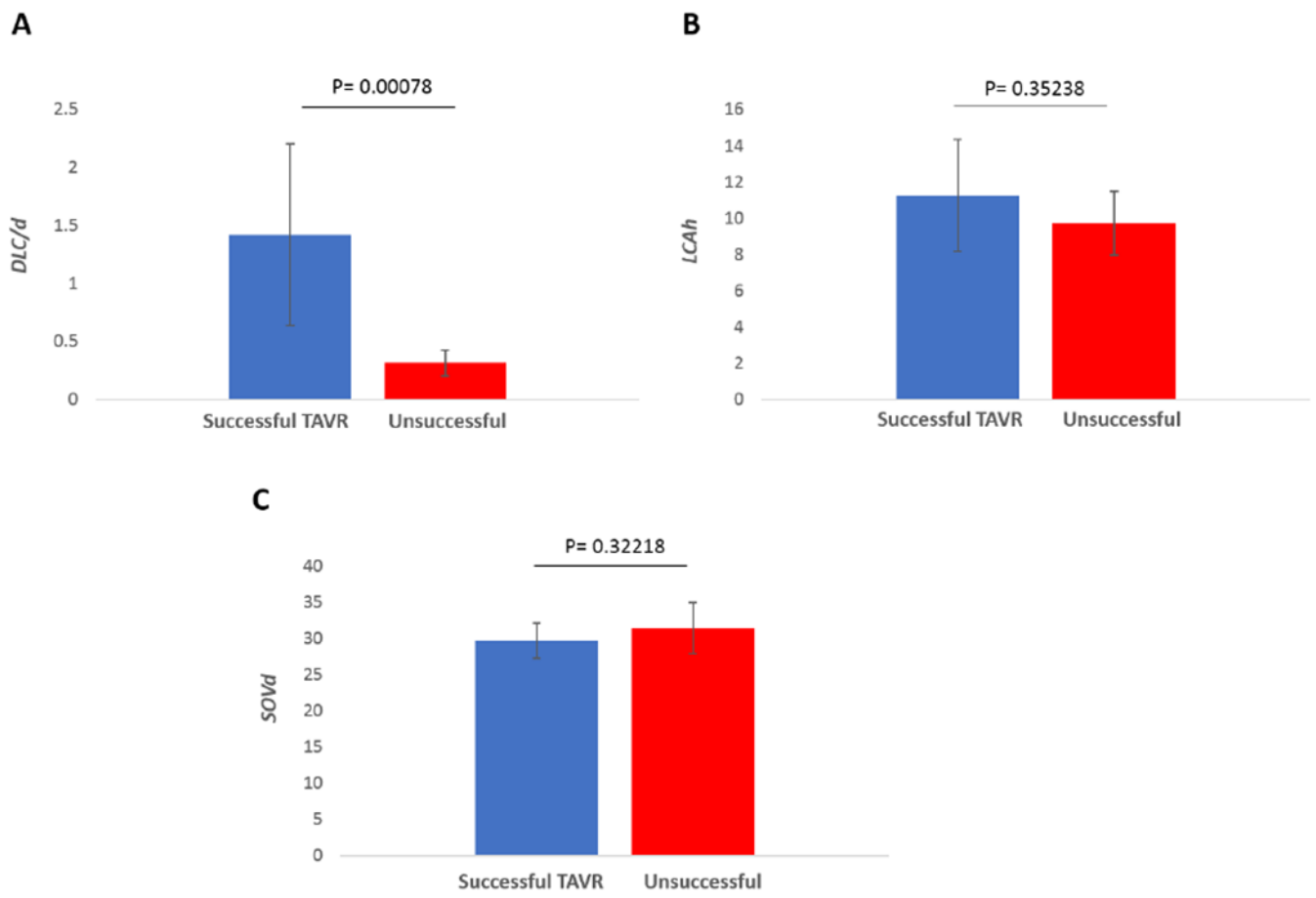

Figure 5.

The mean and standard deviations of the parameter values (*DLC/d,* coronary artery height (*h*) and Sinus of Valsalva diameter (*SOVd*)) for those high risk patients who successfully received a transcatheter aortic valve replacement without coronary obstruction are compared to those who did not receive a transcatheter aortic valve replacement successfully. A significant difference between the two groups was found for the *DLC/d* parameter at significance level 0.05. Neither *h* nor *SOVd* was significantly different between the two groups.

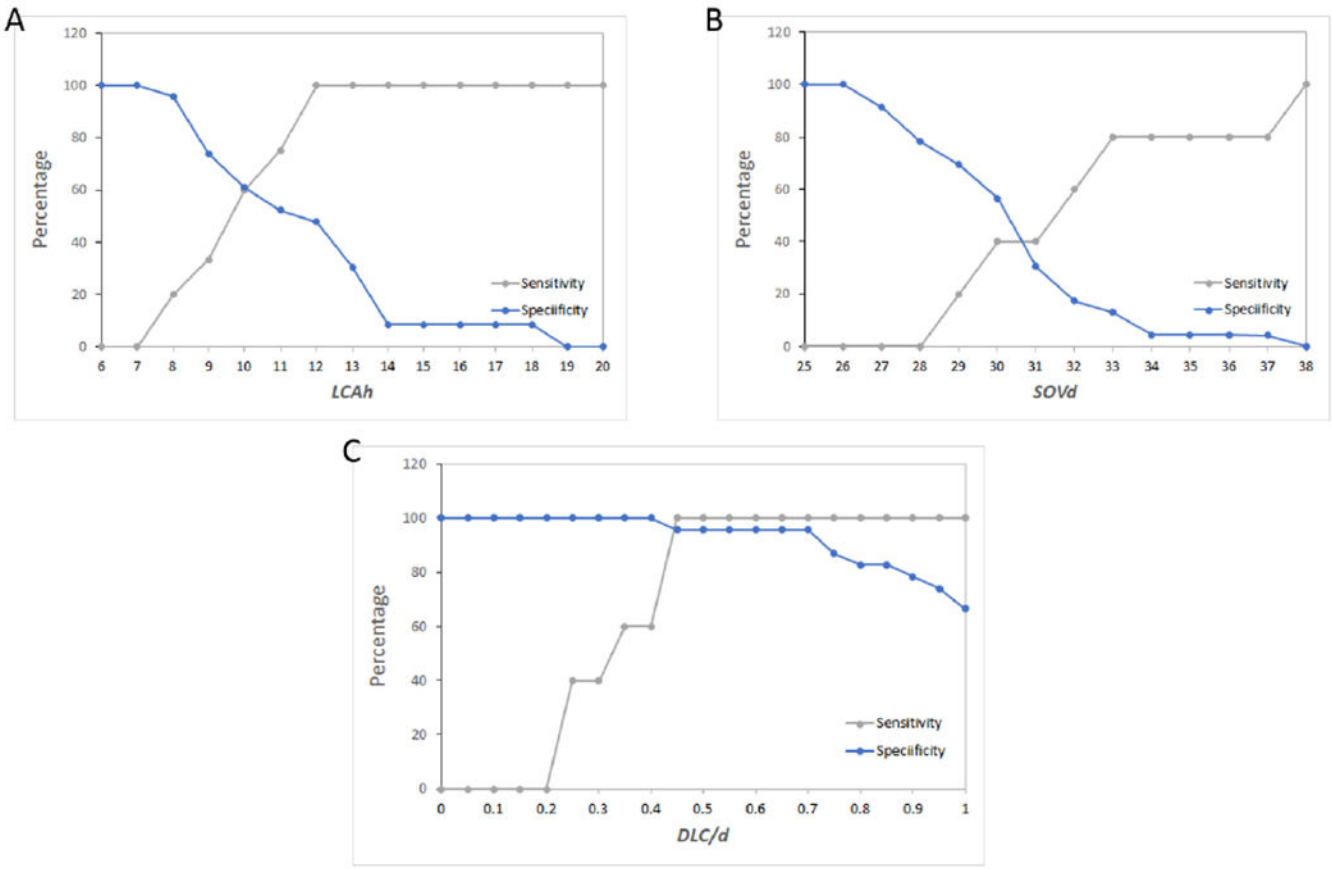

Figure 6.

Sensitivity and specificity curves generated for each of the three parameters (*DLC/d,* coronary artery height (*h*) and Sinus of Valsalva diameter (*SOVd*)) to predict whether transcatheter aortic valve replacement within this high risk patient population would result in coronary obstruction.

Table 1:

List of coronary obstruction predictive parameters including currently used parameters namely coronary ostium height, sinus of Valsalva diameter; and newly proposed predictive parameters based on the 3D computational modeling for each patient.

Patient	Sex	Age	Left Coronary Artery Height (mm)	Sinus of Valsava Diameter (mm)	Left Coronary Artery Diameter (mm)	Valve Diameter (mm)	Simulated TAV Expanded Diameter (mm)	DLC	DLC/d	TAVR Successful?
A	Male	86	13	32	3.62	25	25	3.47	0.96	Yes
B	Female	70	12	27	5.42	23	23	7.44	1.37	Yes
C	Male	88	7.09	36.2	5.3	26	26	2.29	0.43	Yes
D	Female	89	9	30	5.49	23	23	3.85	0.70	Yes
E	Male	93	13	30	2.79	23	23	3.02	1.08	Yes
F	Female	79	10	30	3.31	23	23	3.26	0.98	Yes
G	Female	81	12	29	5.59	26	26	5.69	1.02	Yes
H	Male	94	9	32	4.55	NA	26	0.924	0.20	No
I	Female	81	9	30	3.97	29	29	2.78	0.70	Yes
J	Female	75	9	28	5.72	NA	23	1.16	0.20	No
K	Male	80	12	37	5.43	29	29	1.81	0.33	No
L	Female	68	8	26	4.56	23	23	3.61	0.79	Yes
M	Female	88	13	30	4.97	29	29	7	1.41	Yes
N	Female	91	19	28	3.61	29	29	9.06	2.51	Yes
O	Female	81	8.5	31	3.08	29	29	3.74	1.21	Yes
P	Female	77	8.9	31	3.2	23	23	5.04	1.58	Yes
Q	Female	87	19	27	3.24	20	20	12.6	3.89	Yes
R	Female	74	12	33	4.64	23	23	4.17	0.90	Yes
S	Female	84	9	31	4.24	26	26	6.4	1.51	Yes
T	Female	62	11	29	4.35	NA	23	1.9	0.44	No
U	Female	77	8.5	26	4.19	26	26	3.98	0.95	Yes
V	Female	91	7.6	31	4.59	NA	23	1.84	0.40	No
W	Female	82	11	27	3.18	23	23	3.61	1.14	Yes
X	Female	72	13	29	4.91	26	26	7.92	1.61	Yes
Y	Female	76	12	33	3.39	23	23	4.96	1.46	Yes
Z	Male	61	8.6	29	2.56	26	26	6.98	2.73	Yes
AA	Female	83	10	30	2.8	23	23	3.9	1.39	Yes
AB	Female	77	13	28	2.7	23	23	6.25	2.31	Yes